

## **Annex 5**

# **Optical observations of drop deformation and break-up during emulsification**

Slavka Tcholakova, Nina Vankova, Vassil Vulchev, Nikolai D. Denkov,  
and Ivan. B. Ivanov

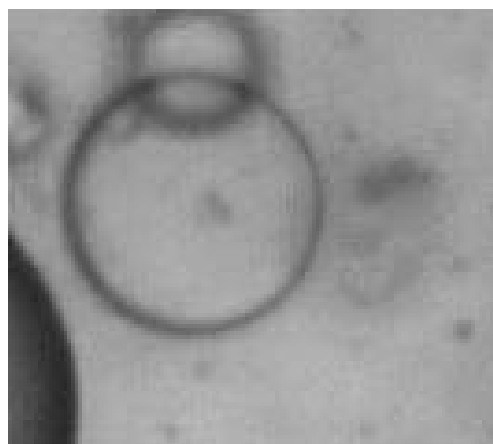
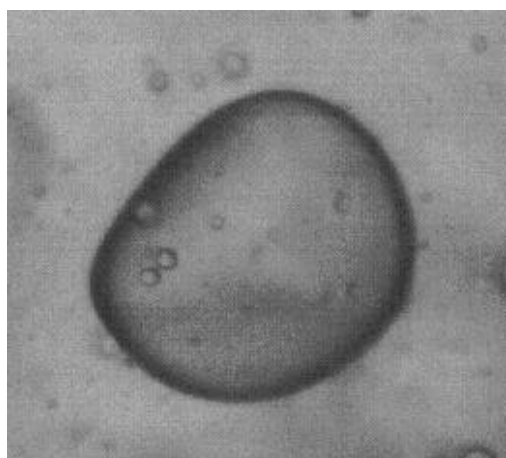
*Laboratory of Chemical Physics & Engineering,  
Faculty of Chemistry, Sofia University, 1164 Sofia, Bulgaria*

In collaboration with Prof. Tomasz Kowalewski and Mr. Slawomir Blonski from IPPT PAN –  
Polish Academy of Sciences, Warsaw, Poland

## ABSTRACT

This part of the report describes optical observations, by a high-speed video camera, of oil drops carried by a turbulent flow. These observations provide information for the drop shape, for the modes of drop disruption and for the drop-drop coalescence (e.g., for the contact time between two drops, formation of films between two drops upon collision, etc.).

To perform such observations we first constructed a new version of the narrow-gap homogenizer, with plane geometry, which allows microscope observations of the drops in turbulent flow. Test experiments were conducted to compare the drop size distribution for emulsions prepared with the new homogenizer having plane geometry and the original homogenizer having cylindrical geometry. These tests showed that the drop-size distribution in emulsions obtained by the two homogenizers are similar, which means that the results from the optical observations with the planar homogenizer can be used to interpret data obtained with the cylindrical homogenizer. Next, preliminary experiments were performed during the visit of Dr. Tcholakova in Warsaw, in collaboration with our Polish partners, to find appropriate experimental conditions for the optical observations. These preliminary experiments provided information about the drop shape in turbulent flow, as well as about the process of drop breakage. Further, more systematic experiments are planned to study the processes of drop breakage and drop-drop coalescence.



Different drop shapes observed in the space just after the processing element; (A) Bulgy type; (B) Lenticular type and (C) Cigar-type.

## 1. Structure of this Chapter.

In this part of the Report we describe the experimental results obtained with the new narrow-gap homogenizer with plane geometry, which allowed optical observations of the motion and shape of drops in turbulent flow. Experiments for comparing the emulsification efficiency of the new homogenizer were carried out in Sofia and are described in section 3 below. Optical observation by a high-speed video camera, of oil drops carried by a turbulent flow, were made in IPPT-Warsaw and a brief description of the main experimental results is given in section 4.

## 2. Materials and methods.

### *1. Materials used for performing the test experiments in Sofia.*

We used three emulsifiers, at high concentrations (1 wt %), to prepare stable oil-in-water emulsions. As a protein emulsifier we used whey protein concentrate (WPC, trade name AMP 8000, product of Proliant) and as low-molecular mass surfactants we used the anionic sodium dodecyl sulfate (SDS, product of Acros). The emulsifiers were used as received. The protein and the surfactant solutions contained inorganic electrolyte NaCl (Merck, analytical grade) with concentration of 150 mM and 10 mM, respectively. The solutions of WPC contained also 0.01 wt % of the antibacterial agent NaN<sub>3</sub> (Riedel-de Haën). All aqueous solutions were prepared with deionized water, purified by a Milli-Q Organex system (Millipore).

As a dispersed phase we used two types of oil, which differ in their chemical composition and viscosity: soybean oil (SBO, commercial product) with viscosity of 50 mPa.s and silicone oil Rhodorsil 621V600 (product of Rhodia), with viscosity of 600 mPa.s. The oils were used as received. The oil viscosity was measured by a Brookfield Rheoset viscometer, see Annex 4, section 5.

### *2. Construction of the homogenization chamber with plane geometry.*

The used experimental cell is equipped with a processing element of plane geometry, ensuring gap-width of 550  $\mu\text{m}$ . Glass windows are mounted at both sides of the cell in such a way, that optical observations could be performed at the position of the gap of the processing element, as well as in the space after the processing element, see Figure 1.

This experimental cell is mounted in the set-up of the modified narrow-gap homogenizer, which is constructed without a pump and allows varying the pressure at the inlet of the chamber (see Chapters 1 and 3 for detailed description).

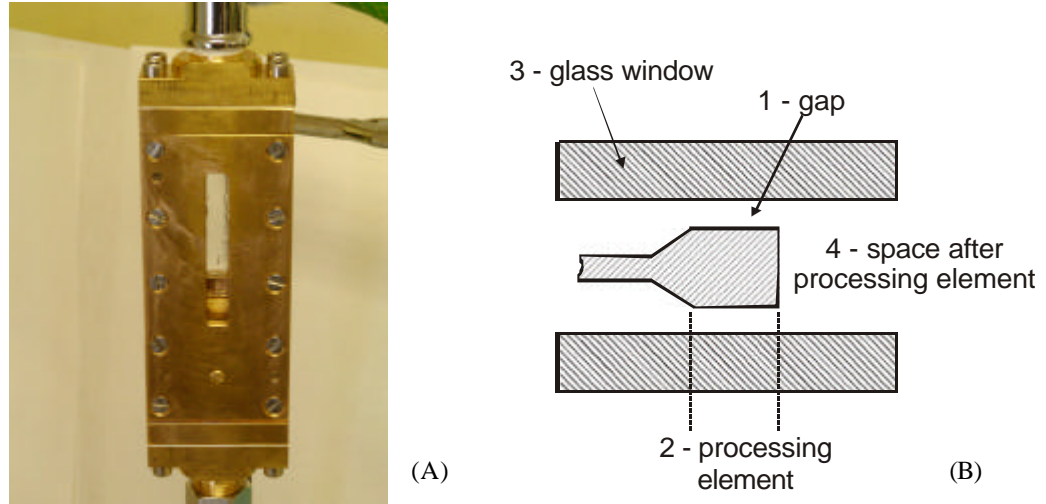


**Figure 1.** (A) Photograph of the new experimental cell with plane geometry; (B) schematic presentation of the space around the processing element.

**Table 1** Operating conditions during emulsification by using the processing element with plane geometry and  $GW = 550 \text{ } \mu\text{m}$ .  $V$  is the mean linear velocity of the fluid,  $p$  is the driving pressure, and  $Q$  is the flow rate.

Studied system	$p \times 10^5$ , Pa	$Q \times 10^{-3}$ , $\text{m}^3/\text{s}$	$V$ , m/s inside the element	$V$ , m/s after the element
1 wt % SDS (10mM NaCl) SBO	0.51	0.12	7.3	1.1
1 wt % WPC (150mM NaCl) SBO	0.52	0.11	6.7	1.0
1 wt % WPC (150mM NaCl) silicone oil	0.48	0.10	6.0	0.92

### 3. Preliminary experiments for comparison of the homogenizers with planar and cylindrical geometry.

First, we tested the new experimental cell (processing element with plane geometry) by performing experiments with different systems in the so-called “surfactant-rich” regime [1-3], in which the drop-drop coalescence is negligible and the mean drop-size is determined by the drop breakage process only. As mentioned in section 1.1, we used two types of emulsifiers, WPC and SDS, both in concentration of 1 wt %, to stabilize the emulsions. We performed preliminary experiments with one emulsion stabilized by SDS (+ 10 mM NaCl) and two WPC-stabilized emulsions (+ 150 mM NaCl), using SBO as an oil phase at two

different volume fractions:  $\Phi = 0.05$  and  $0.28$ . Silicone oil with viscosity of  $600 \text{ mPa.s}$ , at  $\Phi = 0.05$ , was used for preparation of one emulsion, stabilized by WPC (+  $150 \text{ mM NaCl}$ ). The emulsification was carried out at a low driving pressure,  $p \approx 0.52 \times 10^5 \text{ Pa}$  (the exact pressure values for each emulsion are given in Table 1). The experimental results for  $d_{32}$ , after the  $10^{\text{th}}$  pass through the processing element, are presented in Table

**Table 2.** Mean volume-surface diameter,  $d_{32}$ , for the studied SDS- and WPC-stabilized emulsions of SBO with  $\eta_D = 50 \text{ mPa.s}$  ( $\Phi = 0.05$  and  $0.28$ ) and of silicone oil with  $\eta_D = 600 \text{ mPa.s}$  ( $\Phi = 0.05$ ). The emulsification is performed at  $p \approx 0.52 \times 10^5 \text{ Pa}$ , by using the processing element with plane geometry and  $\text{GW} = 550 \mu\text{m}$ .

Aqueous phase	Oil phase	$\eta_D$ , mPa.s	$\Phi$	$d_{32}$ , $\mu\text{m}$ (10 passes)
1 wt % SDS (+ $10 \text{ mM NaCl}$ )	SBO	50	0.28	10.3
1 wt % WPC (+ $150 \text{ mM NaCl}$ )	SBO	50	0.05	24.5
	SBO	50	0.28	38.0
1 wt % WPC (+ $150 \text{ mM NaCl}$ )	silicone oil	600	0.05	50 – 100

As seen from Table 2, we managed to produce stable oil-in-water emulsions with all studied systems. The mean drop size of the SBO-emulsions, stabilized by WPC, was larger than that of the SDS-stabilized emulsion, because the interfacial tension,  $\sigma_{OW}$ , of the protein solution was larger ( $\approx 10 \text{ mN/m}$ ) than that of the SDS-solution ( $\approx 4 \text{ mN/m}$ ). The results show that the narrow-gap homogenizer with plane geometry of the mixing chamber works well for emulsification of various systems.

For optical observations of the emulsification process, the emulsion prepared with silicone oil of viscosity of  $600 \text{ mPa.s}$  (at  $\Phi = 0.05$ ) and aqueous solution of 1 wt % WPC (+  $150 \text{ mM NaCl}$ ), was found to be suitable. Only this system contained a large fraction of drops, whose diameters fell in the range between  $50$  and  $100 \mu\text{m}$ , and were appropriate for optical observations.

#### 4. Optical observations of drops in turbulent flow.

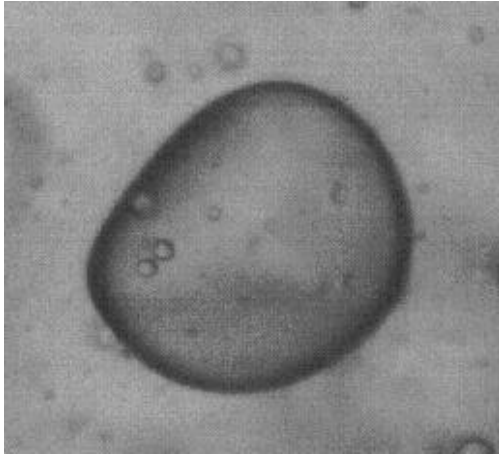
In this series of experiments we used silicone oil with viscosity  $500 \text{ mPa.s}$  as a dispersed phase and 1 wt % solution of Brij 58 as a continuous phase. This concentration of Brij 58 is sufficient to prevent the drop-drop coalescence and only the processes of drop deformation and breakage are observed during emulsification. The experiments are performed in IPPT-Warsaw and high-speed camera model PCO.1200hs (product of Samwoo Scientific Co.) is used for recording the pictures. The applied pressure was around  $0.5 \text{ atm}$  and the flow

rate was around 0.062 L/s. The comparison of the mean drops size for emulsions prepared with narrow-gap homogenizer with cylindrical geometry and that with plane geometry allowed as to estimate the volume, in which the turbulent energy dissipation takes place. The comparison of the experimental results obtained on the two homogenizers with 1 wt % WPC and SBO showed that the volume, in which the dissipation of energy takes place in the planar homogenizer is around  $5 \times 10^{-7} \text{ m}^3$ , which corresponds to rate of energy dissipation  $\approx 10^6 \text{ J/m}^3 \cdot \text{s}$ . Substituting this value in eq 1.2, and taking into account that  $\sigma_{OW} \sim 10 \text{ mN/m}$ , we estimate that the maximal diameter of stable drops,  $d_K$ , is around 50  $\mu\text{m}$  under these experimental conditions. From the geometrical parameters of the system we estimate that the average linear velocity of the fluid through the gap of the processing element is around 3.7 m/s, whereas after the processing element it is around 0.5 m/s. We were unable to observe the motion of drops in the gap of processing element, and for this reason, the observations are made just after the processing element, as well as at 1, 5 and 4 cm after the processing element, see Figure 1B.

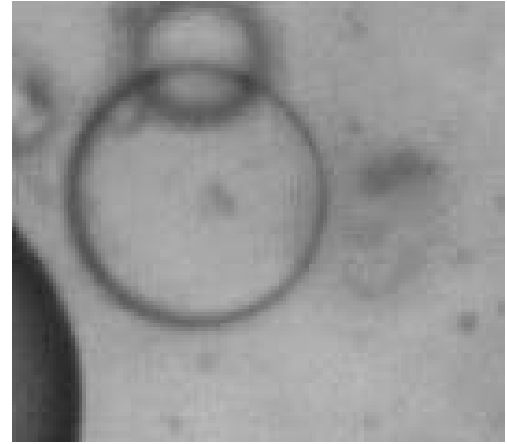
#### **4.1. Optical observations made just after the processing element.**

The motion of the drops in the space just after the processing element is very intensive and irregular, which makes difficult to recognize a given drop in two consecutive video frames. The used camera takes around 700 frames per seconds, which means that the time between two consecutive pictures is around 1.4 ms. For most of the performed experiments, this time was too long and we were unable to recognize a given drop on two consecutive pictures. That is why, this series of experiments allowed us to observe the shape of the drops only. The main observations can be summarized in the following way, see Figure 2-5:

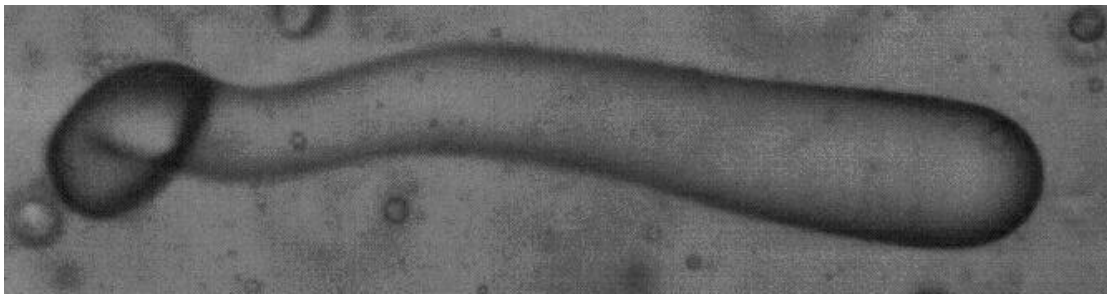
- Three different types of drop shapes are observed - bulgy (see Figure 2A), lenticular (see Figure 2B) and cigar-shaped (see Figure 2C). The deformation of type “bulgy” is known to appear only as a result of the dynamic pressures in turbulent flow, as explained by Hinze [4]. This drop shape indicates that we have intensive turbulent flow in the space just after the processing elements. The other two observed shapes, cigar-type and lenticular, indicate that hyperbolic and Couette-type local flow patterns appear in this region of the homogenizer [4].



(A)



(B)



(C)

**Figure 2.** Different drop shapes observed in the space just after the processing element; (A) Bulgy type; (B) Lenticular type and (C) Cigar-type.

- In some of the experiments we were able to record pictures of drops in the process of their break-up, see Figure 3. The breakage process leads to formation of drops with different sizes and different number of daughter drops, depending on the type of drop deformation.
- For drops with lenticular deformation we observed that their breakage often leads to formation of around 2 to 5 drops with different diameters plus a significant number of very small drops, see Figure 3. The smallest drops are formed by a Rayleigh type of capillary instability of thread-like filaments, which form in the process of breakage of the original large drop. These very small drops are often called “satellite drops” in the literature [4-5].
- The drops with lenticular shape seem to deform and break easier than those having cigar- and bulgy shapes, see Figure 4
- Collisions between drops are recorded in some pictures, which indicate that we might be able to observe the process of drop-drop coalescence at lower surfactant concentration.
- Some of the drops having cigar shape restore their spherical shape without breakage, even if the initial aspect ratio is more than 10.
- Almost all drops having diameter above 50  $\mu\text{m}$  have irregular shape, which shows that all drops with diameter larger than  $d_K$  are deformed, see Figure 5.

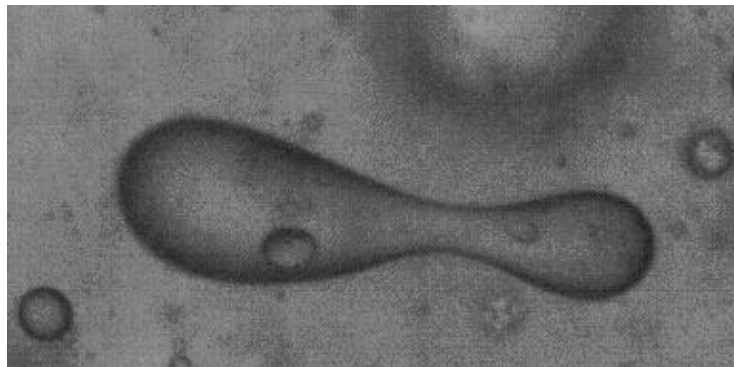
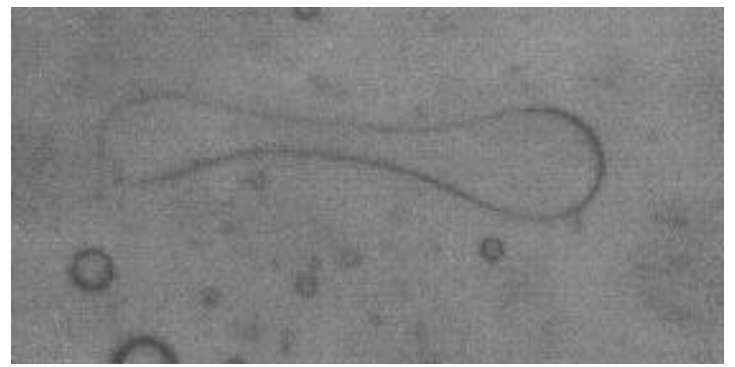
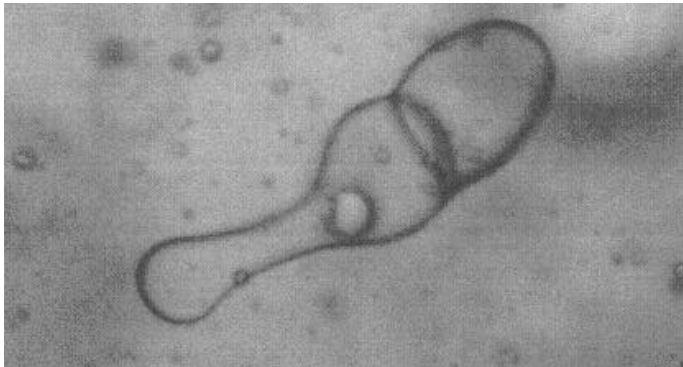
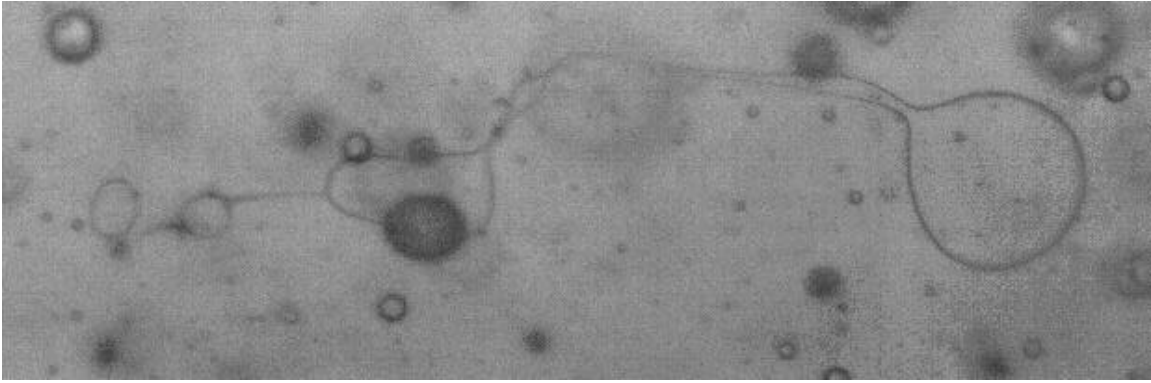
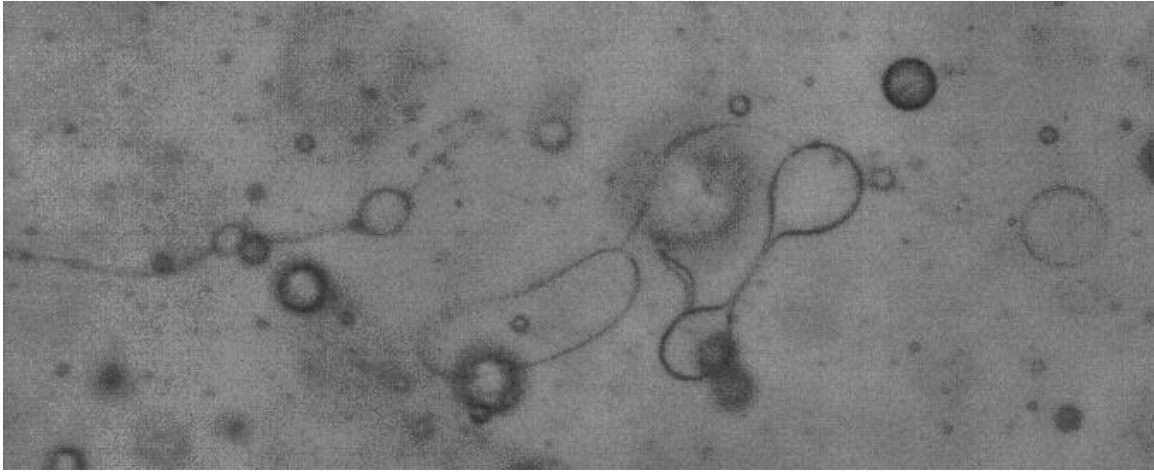
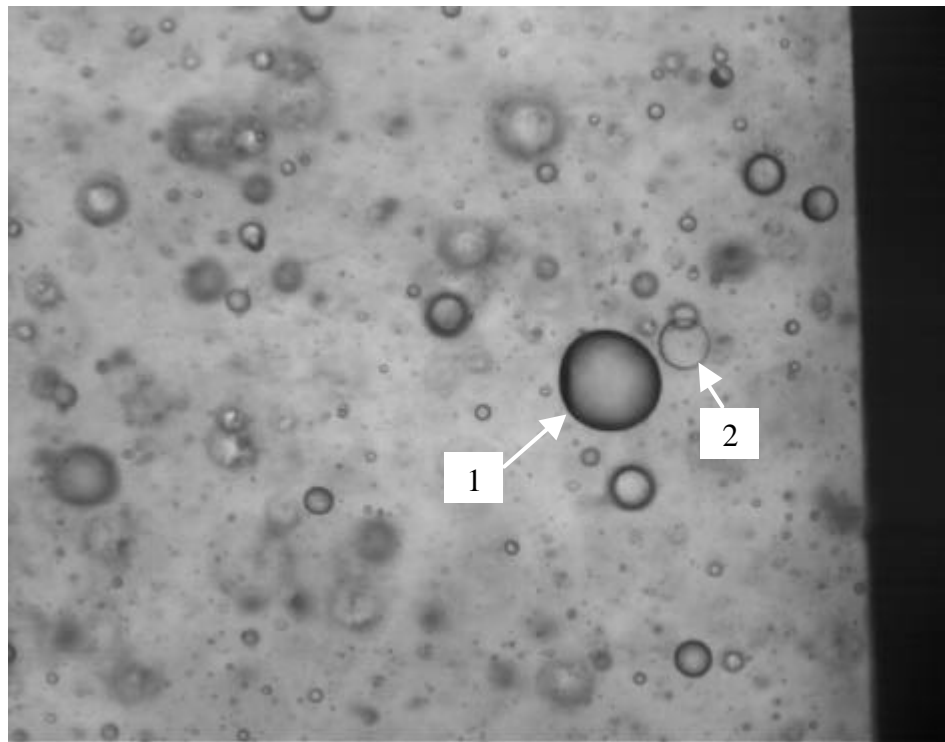
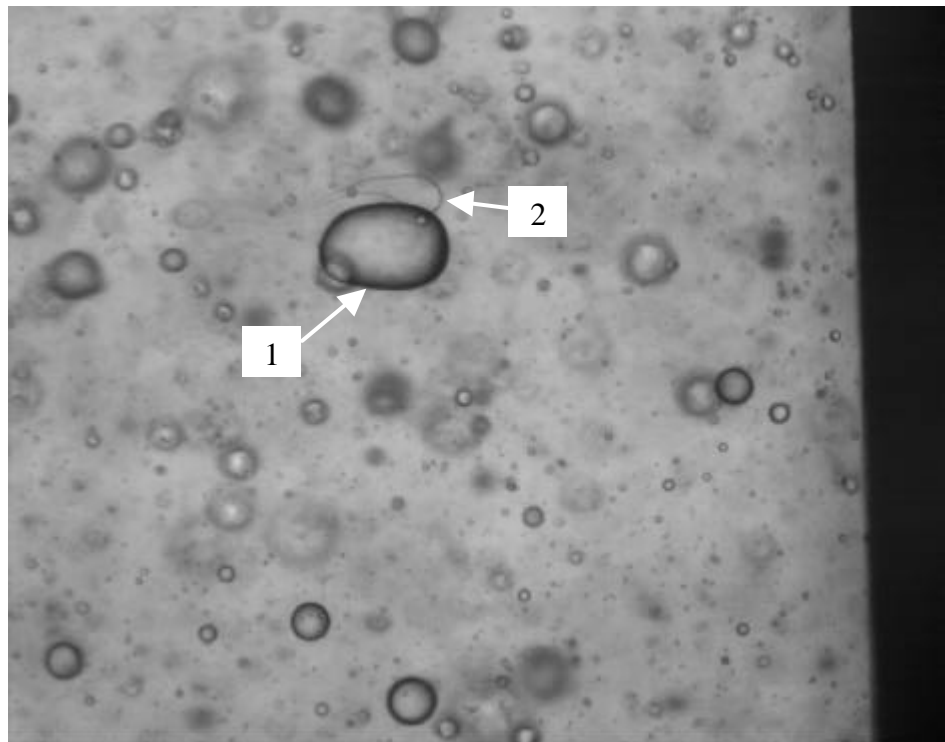


**Figure 3.** Drops in the course of their breakage in turbulent flow – the pictures are recorded in the region just after the processing element.

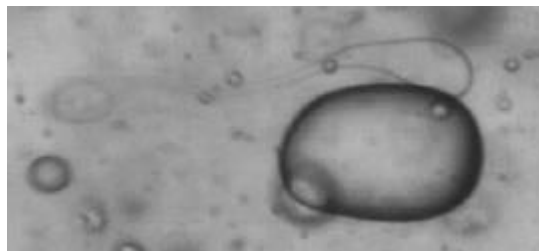




(A)



(B)



(C)

**Figure 4.** (A,B) Two consecutive pictures taken in the space just after the processing element. The picture in (C) shows a magnified view of the breaking drop from (B).

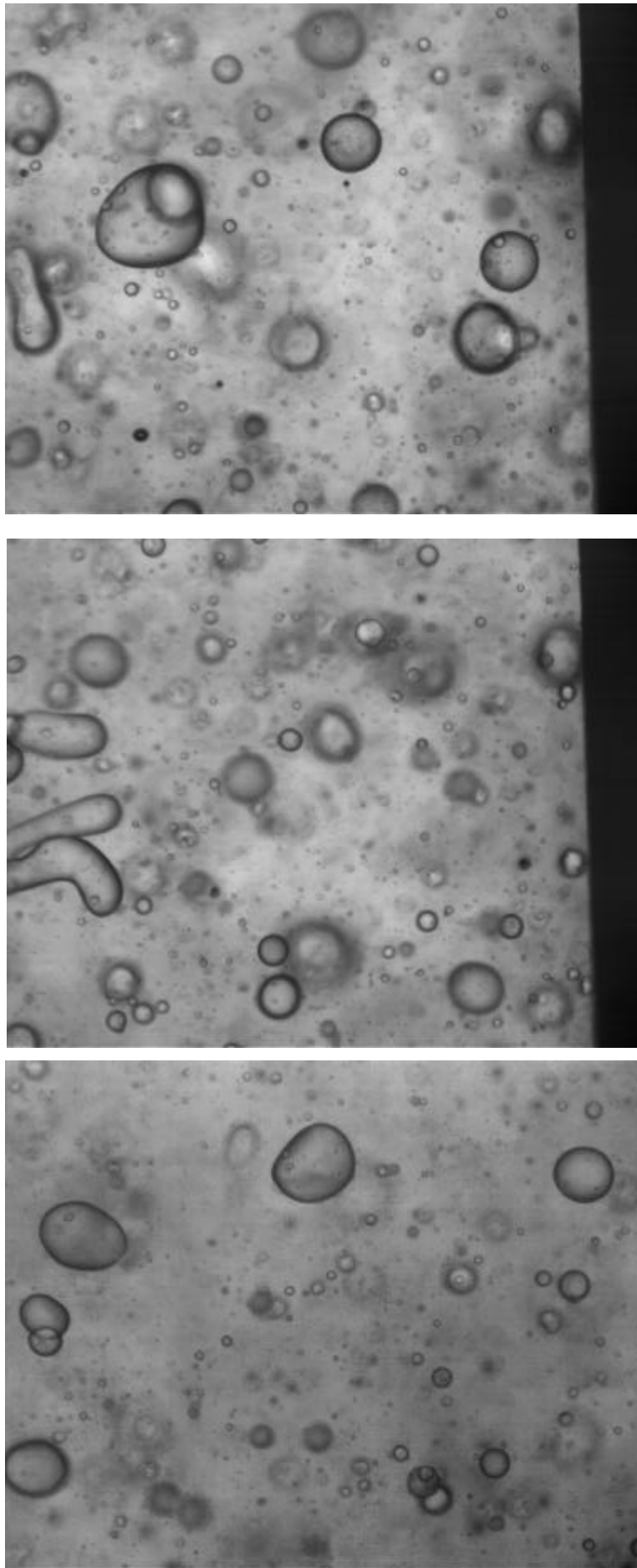


**Figure 5.** Pictures recorded in the space just after the processing element.

#### 4.2. Optical observations made 1 cm after the processing element.

In this region of the homogenizer we were able to recognize a given drop in two consecutive frames. From drop displacement we can estimate roughly the average linear velocity of the fluid to be around 2 m/s, see Figure 6. The drop deformation is smaller in this region, cf. Figures 5 and 6. The drops with diameter smaller than 150  $\mu\text{m}$  are more or less of spherical shape. If one assumes that the pressure fluctuations are smaller than in the space just after the processing element, one can estimate the time required for relaxation of the drop shape to spherical one (by comparing it to the time required for traveling of a drop from the processing element to the observed region). The relaxation time of the drop shape is given by the relation [5,6]

$$t_{REL} = \frac{\eta_D d}{\sigma_{OW}} \quad (1)$$

where  $\eta_D$  is the oil viscosity, 500 mPa.s,  $d$  is drop diameter, and  $\sigma_{OW}$  is interfacial tension (10 mN/m for the studied system). The estimate show that  $t_{REL}$  for drops with diameter 100  $\mu\text{m}$  is expected to be around 5 ms. If one assumes that the drop linear velocity is around 2 m/s (as estimated from the video-records), the time required for their traveling of 1 cm is around 5 ms, which is comparable with the relaxation time. This comparison of the relaxation and traveling times explains why drops with diameter of  $\approx 100 \mu\text{m}$  have approximately spherical shape – they have had sufficient time to relax. The larger drops do not relax to the spherical shape, which could be due to their longer relaxation time or to the possibility that the pressure fluctuations in this region are sufficiently large to deform these drops.

It is interesting to note that cigar shape deformation is not observed in this region of the homogenizer. Furthermore, we do not observe any breaking drops here. The bulgy type deformation is mostly observed in this region, which could be due to the action of pressure fluctuations or to the longer relaxation time for the larger drops, as predicted by eq 1.

In conclusion, most of the drops with diameter below 150  $\mu\text{m}$  restored their spherical shape and the cigar shape deformation is observed only occasionally. The observations show that the process of drop-drop coalescence could be, probably, observable in this region with appropriate systems.

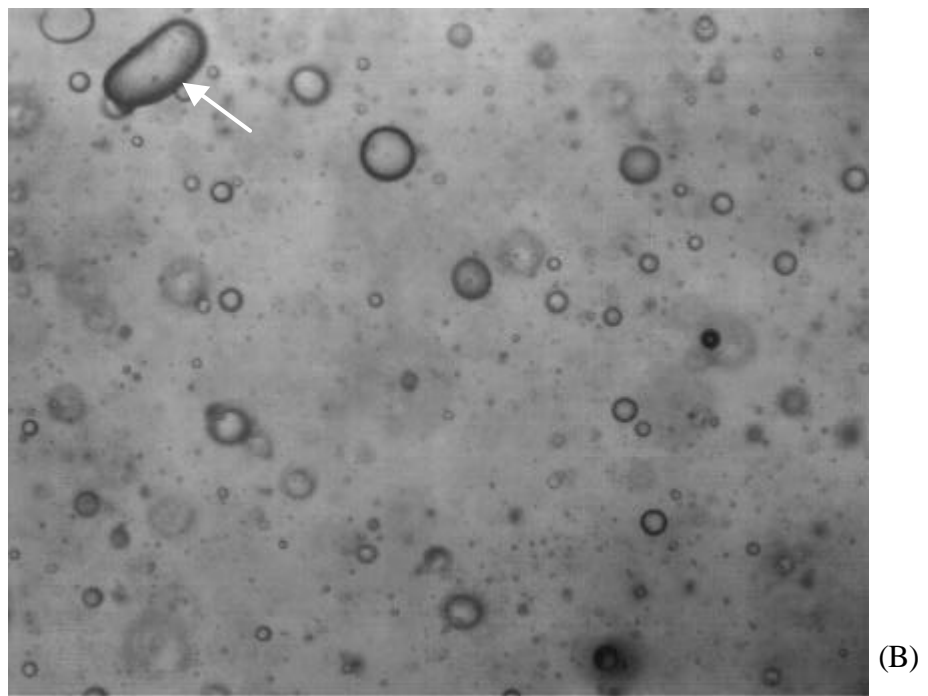
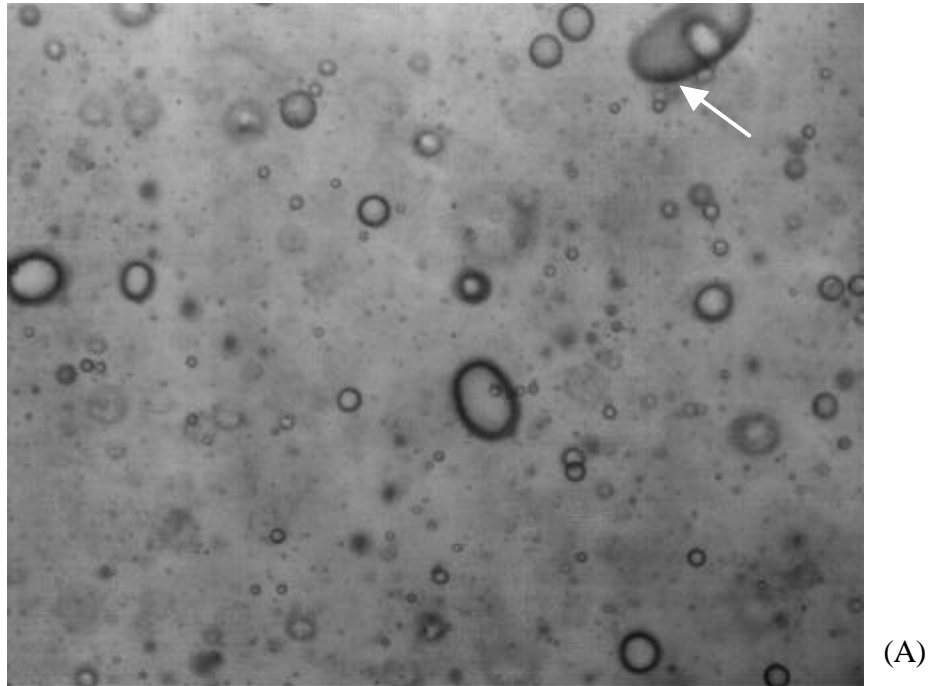


**Figure 6.** Two consecutive pictures made at 1 cm after the processing element. The arrow points to a drop traveling along the observation area.

#### 4.3. Optical observations made at 5 cm after the processing element.

In this region the drops have much lower velocity and a given drop can be captured in 3-5 consecutive frames, see Figure 7. From the drop displacements we estimate roughly that the average velocity of the fluid is around 0.5 m/s. However, some of the drops move in irregular way, around a given position for relatively long time, as illustrated in the consecutive pictures presented in Figure 7. In this region, most of the drops with diameter above 250  $\mu\text{m}$  are spherical, whereas the larger drops are slightly deformed with bulgy shape. The cigar shape deformation and lenticular deformation are not observed.

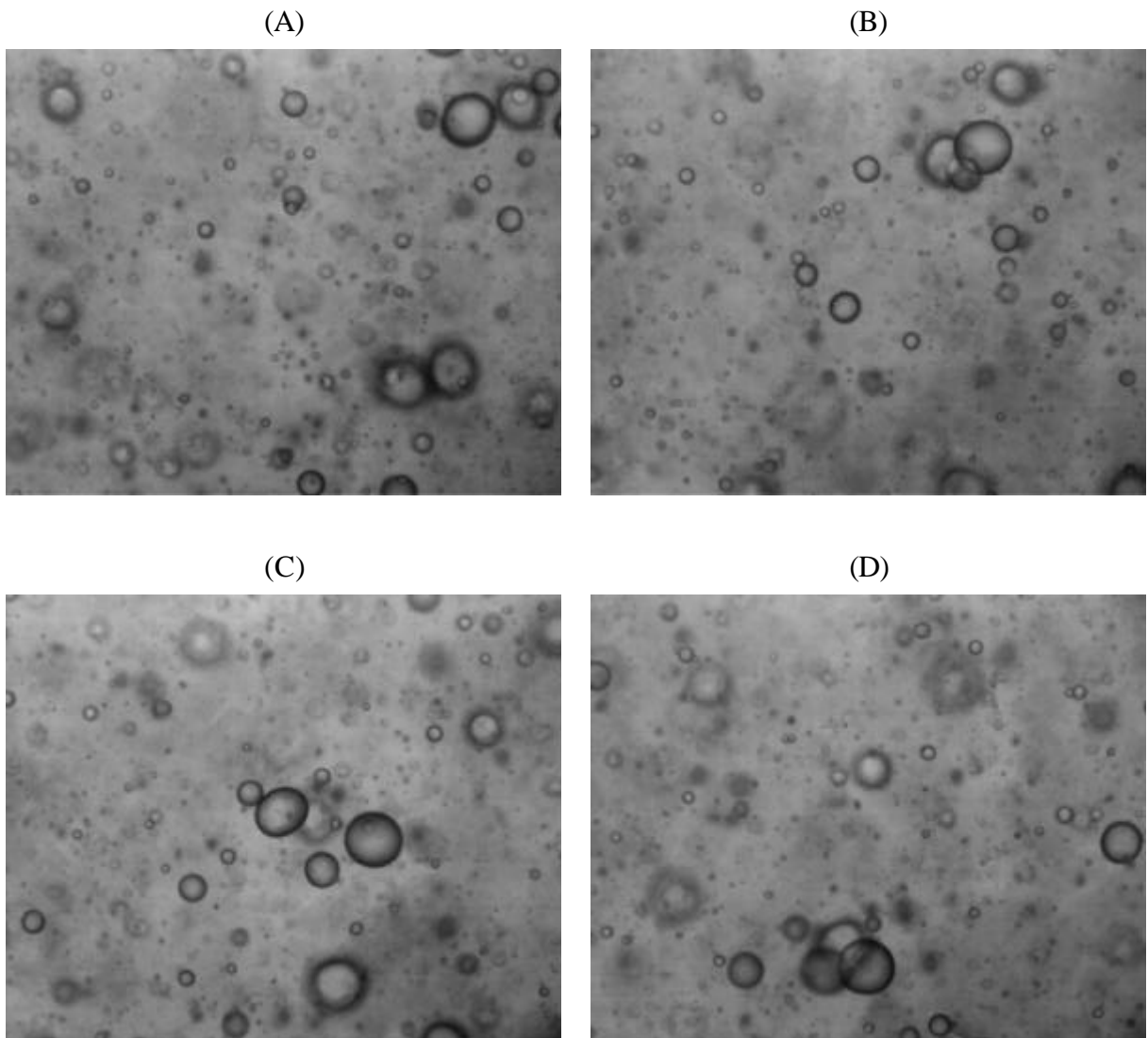


**Figure 7.** Consecutive pictures taken at 5 cm after the processing element.

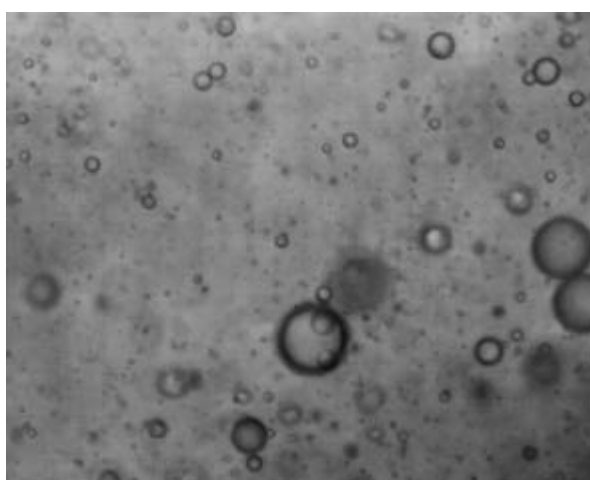
#### **4.4. Optical observations made at 4 cm after the processing element.**

In this region, the drop motion is almost regular, which is indicated by the fact that the drops captured in consecutive frames remain almost at the same focus in all consecutive pictures, see Figure 8. The average velocity estimated from drop motion is around 0.3 m/s. Almost all drops have spherical shape and only the biggest ones, with diameter above 600  $\mu\text{m}$ , are slightly deformed. The estimate of the relaxation time of 600  $\mu\text{m}$  drops, by eq 1, shows that it is around 30 ms, whereas the average time required for traveling the drops from the processing element to this place is around 80 ms.

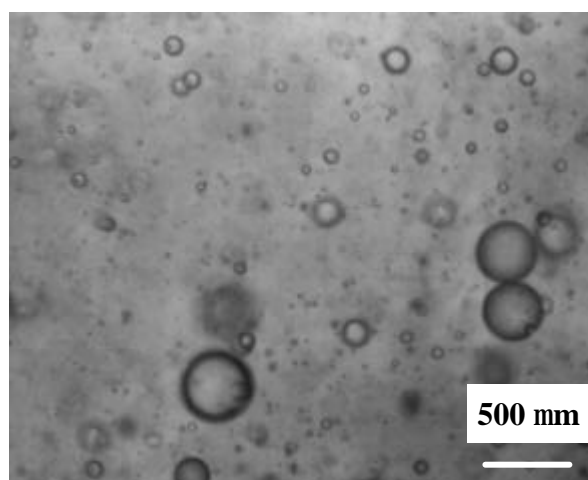
Formation of doublets of drops is observed in some pictures – the drops move together for 2-3 ms and then separate, see Figure 8. From such pictures we could estimate the contact time of the drops (2-3 ms for the drops shown in Figure 8). The formation of a film between colliding drops could be also recognized in some of the pictures.

#### **5. Conclusions:**

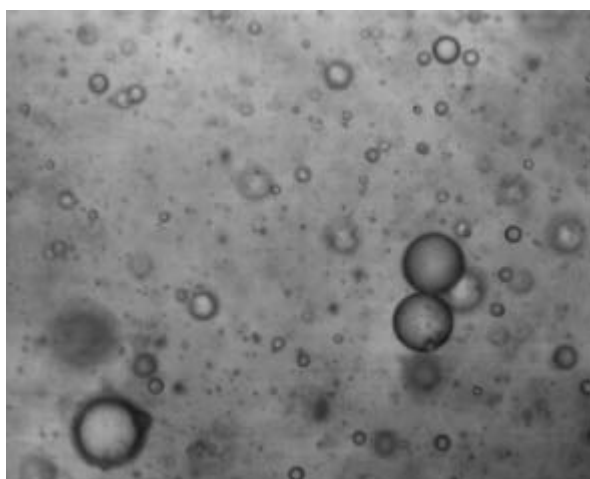
1. An experimental cell with planar geometry is constructed and tested, which allows optical observations of the drops in the homogenizer.
2. Experiments aimed to compare the new experimental cell with the previous one are performed. The results show that the mean drop size is similar for both homogenizers (with plane and with conical constructions).
3. Preliminary experiments with direct observation of the motion and shape of the drops in the homogenizer show that:
  - The drops are strongly deformed in the region just after the processing element and they restore their spherical shape when they move away from the processing element. The drop relaxation is approximately described by eq 1.
  - Three types of deformed drops are observed in the region just after the processing element: cigar-type, lenticular type and bulgy. These three types of deformation are the most probable ones for turbulent flow, according to Hinze [4].
  - The breakage process depends on the type of drop deformation and, typically, leads to formation of 2-5 smaller drops and a large number of satellite drops.



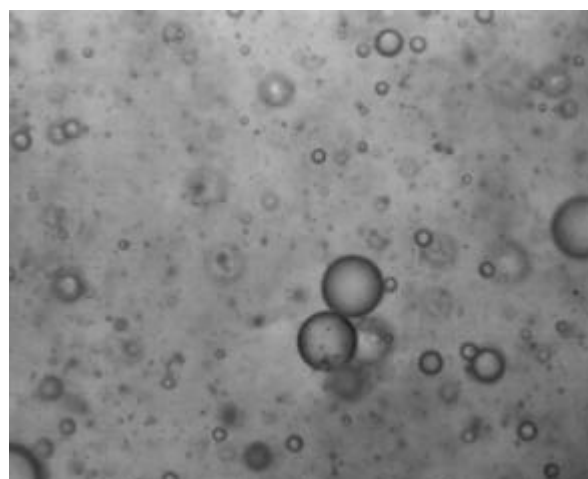
(A)



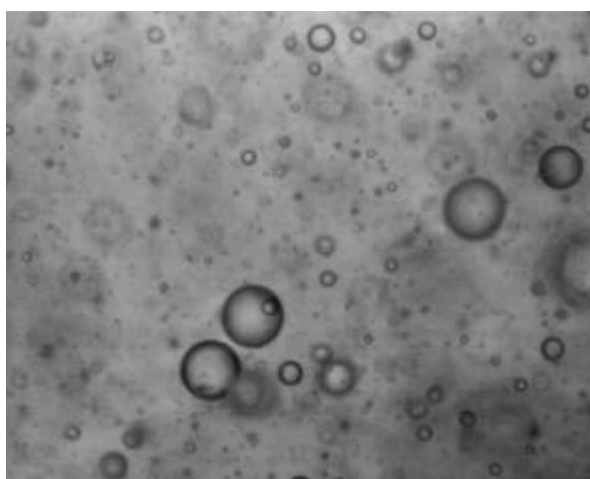
(B)



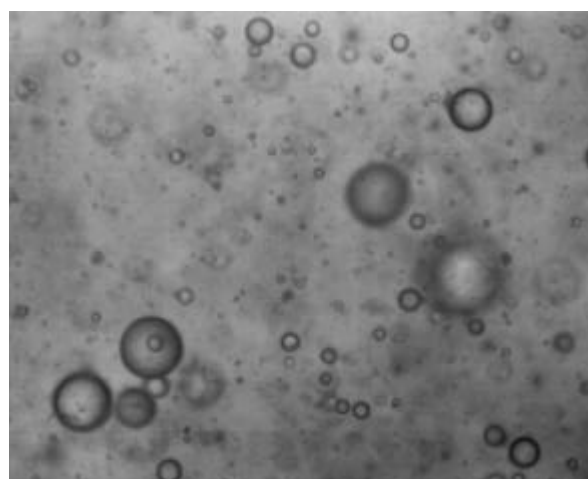
(C)



(D)



(E)



(F)

**Figure 8.** Consecutive pictures taken at 4 cm after the processing element.

### **References:**

1. Taisne, L.; Walstra, P.; Cabane, B. Transfer of oil between emulsion droplets. *J. Colloid Interface Sci.* **1996**, *184*, 378.
2. Tcholakova, S.; Denkov, N. D.; Danner, T. Role of surfactant type and concentration for the mean drop size during emulsification in turbulent flow. *Langmuir* **2004**, *20*, 7444-7458.
3. Tcholakova, S.; Denkov, N. D.; Sidzhakova, D.; Ivanov, I. B.; Campbell, B. Interrelation between drop size and protein adsorption at various emulsification conditions. *Langmuir* **2003**, *19*, 5640-5649.
4. Hinze, J. O. Fundamentals of the hydrodynamic mechanism of splitting up in dispersion processes. *AIChE Journal* **1955**, *1*, 289.
5. Stone, H. A. Dynamics of drop deformation and breakup in viscous fluids. *Annu. Rev. Fluid Mech.* **1994**, *26*, 65.
6. Hu, Y. T.; Lips, A. Determination of viscosity from drop deformation. *J. Rheol.* **2001**, *45*, 1.